Isolation and Characterization of Microfibrillated Cellulose from Agro-industrial Soybean Residue (Okara)

Peiyi Li,[a,b,c,d,]* Yumeng Wang,[a] Qingqing Hou,[a] and Xinping Li [a,c,d]

Microfibrillated cellulose (MFC) was isolated from the byproduct of soymilk, tofu, and okara (soybean residue) using a chemi-mechanical technique. Initially, petroleum ether treatment at 50 °C for 8 h and protease treatment at 50 °C for 2 h were used to remove fat and protein, respectively. A 6 wt% hydrochloric acid solution at a 20 mL/g acid-to-cellulose ratio was applied at 88 °C for 60 min to remove the residual hemicellulose and degrade cellulose. Finally, the sample was gently homogenized at 60 MPa to aid in individualization of the fibers to nano dimension; homogenization for 5 and 25 passes resulted in fibers labeled as MFC-5 and MFC-25, respectively. The amorphous region of okara cellulose was higher than other non-wood fibers. The average diameters of MFC-5 and MFC-25 were within the range of 13 nm to 93 nm and 9 nm to 55 nm, respectively. MFC obtained from okara has potential to reinforce ecofriendly cellulosic nanofibrillated for diverse applications.

Keywords: Microfibrillated cellulose; Okara (soybean residue); Agro-industrial waste; Characterization

Contact information: a: College of Bioresources Chemical and Materials Engineering, National Demonstration Center for Experimental Light Chemistry Engineering Education, Shaanxi University of Science and Technology, Xi'an 710021, China; b: Tianjin Key Laboratory of Pulp and Paper, Tianjin University of Science and Technology, Tianjin, 300457, China; c: Key Laboratory of Paper Based Functional Materials of China National Light Industry, Xi'an 710021, China; d: Shaanxi Provincial Key Laboratory of Papermaking Technology and Specialty Paper Development, Xi'an 710021, China;
** Corresponding author: lipeiyi@sust.edu.cn*

INTRODUCTION

Microfibrillated cellulose (MFC), also called cellulose nanofibers (CNF) or nanofiber cellulose (NFC), is a functional, nanometer-grade material with wide applications. MFC is a material composed of nanosized cellulose wireline microfibers. Typical microfiber widths are 5 nm to 60 nm with a wide range of lengths, typically several micrometers (Klemm *et al.* 2011). Due to the high specific surface area, broad possibility of surface modification (Eichhorn *et al.* 2010), barrier properties, high mechanical strength (Ferguson 2012), and safety aspects (Vartiainen *et al.* 2011), MFC is a promising biomaterial for use in bio-nanocomposites, paper and paperboard (Missoum *et al.* 2013), food, hygiene and absorbent products, emulsion and dispersion (Xhanari *et al.* 2011), medical, cosmetic and pharmaceutical products (Syverud *et al.* 2011), and other applications (Nyström *et al.* 2015).

MFC has been isolated from various cellulosic sources, including bleached kraft pulp (Spence *et al.* 2010a, b), bleached sulfite pulp, bamboo pulp (Zhang *et al.* 2015), miscanthus straw residue (Henniges *et al.* 2014), rice straw (Hassan 2015), wheat straw (Singh *et al.* 2016), cocoa pod husk (Jimat and Zailani 2016), sugarcane bagasse (Petroudy *et al.* 2014), sugar beet pulp (Agoda-Tandjawa *et al.* 2010), corn cobs (Shogren *et al.* 2011), prickly pear fruit peels (Habibi *et al.* 2009), and Japanese cedar (Shi *et al.* 2015).

Additionally, raw banana, pineapple leaf fibers, basts of flax, hemp, jute, and leaves of sisal and abaca have been explored to produce MFC (Alila *et al.* 2013). Although wood is the main raw material that has been used in the production of MFC (Lavoine *et al.* 2012), the demand of non-wood resources (such as agricultural crops and their by-products) has increased with the competition among many other fields that use wood.

Soybean residue (SR), an agricultural waste, is produced during the processing of soybean products and remains after the water-soluble fraction is filtered in the making of soymilk and tofu (Vong and Liu 2017). However, the average composition of okara includes approximately 50% to 60% carbohydrate, 15% to 30% protein, 5% to 20% fat, and 3% ash (Vong and Liu 2016). It is very huge, low cost, and renewable resource. At present, only a small part of SR is used for food consumption, and most of it is used for the feed or is abandoned directly (Zhao *et al.* 2013), which has caused a great waste of resources and environmental pollution. SR is a suitable substrate for producing a variety of functional foods, biomaterials, value-added chemicals, and biofuels (Abdulkhani *et al.* 2017). SR is the parenchymal tissue; whose cell wall is thin and the binding force between microfibrils is small. Such properties are beneficial to the preparation of MFC by mechanical treatment. SR has been used to product nanocellulose by acid hydrolysis followed by high-pressure homogenization (Liu *et al.* 2012). However, acid hydrolysis and homogenization do not produce okara cellulose nanofibrils with a uniform size distribution. Furthermore, due to a lack of purification of okara, it only can produce nanoparticles rather than nanocellulose. Consequently, okara needs an effective treatment is to produce well-separated nanofibrillated cellulose with a proper morphology.

In this study, a chemical treatment together with a mechanical treatment was used for MFC production from okara. This work explored the feasibility of using okara as a new potential cellulosic precursor for production of MFC to convert this waste into value-added products. MFC was isolated from okara by chemi-mechanical methods. The cellulose, holocelluloses, protein, fat, and lignin contents of the processed nanofibers were determined by chemical analysis. The morphology of the nanofibers was investigated by scanning electron microscopy. Fourier Transform infrared spectroscopy (FTIR) spectroscopy, X-ray diffraction (XRD), and Thermogravimetric Analysis (TGA) experiments were performed to characterize the processed nanofibers.

EXPERIMENTAL

Materials

Okara that was used as raw material was obtained from a soymilk mill in China and was dried to 10% moisture. Petroleum ether (boiling range 30 °C to 60 °C), sodium hydroxide, sodium chlorite, and glacial acetic acid was purchased from the Tianjin Damao Chemical Reagent (Tianjin, China). Analytical grade hydrochloric acid (36% to 38%) was obtained from the Sinopharm Chemical Reagent (Beijing, China). Protease was purchased from Shenzhen Leveking Bio-Engineering (Shenzhen, China). Deionized water was used in all experiments, and the samples were stored in the desiccator at the room temperature until used.

Extraction of Microfibrillated Cellulose

Purification

The non-cellulosic components in okara were removed to isolate cellulose. The okara (SR) powder was first washed 5 to 6 times with warm distilled water to remove aqueous soluble substances, and then it was oven-dried at 55 °C for 24 h. The okara powder was extracted with petroleum ether at 50 °C for 8 h to remove the fat, followed by oven-drying at 55 °C for 24 h. The protein in the okara was removed with 1.5% (w/w) protease at 50 °C for 2 h, and then it was inactivated in a boiling water bath for 10 min.

Hydrochloric acid treatment

The aqueous sample suspension was centrifuged and filtrated with deionized water. The sample was hydrolyzed using 6 wt% hydrochloric acid at a 20 mL/g acid-to-cellulose ratio at 88 °C for 60 min. To stop acid hydrolysis, five volumes of cold water were added. The suspension was washed with distilled water until the filtrate reached neutral pH and then was freeze-dried for 12 h to remove water. The extracted material was the treated okara (TSR).

Homogenization treatment

Cellulose isolated from okara was homogenized using a HP-4 L high-pressure homogenizer (Xigao, China) operated at 60 MPa. The suspension consistency during homogenization was 1%. MFC-5 and MFC-25 samples were collected after 5 passes and 25 passes, respectively, and then were freeze-dried for 12 h to remove water.

Characterization of Microfibrillated Cellulose

Chemical analysis

The holocellulose in fibers was determined using a $NaClO_3$ and NaOH mixture, as previously described (Zobel and McElwee 1958). The α-cellulose content of the fibers was then calculated by further NaOH treatment to remove the hemicelluloses. The difference between the values of holocellulose and a-cellulose can be used to estimate the content of the hemicellulose (Alemdar and Sain 2008). The chemical components in SR and TSR were determined according to the following standards: ash (TAPPI T211 om-02 2011), lignin (TAPPI T222 om-11 2011), fat (GB/T 5009.6 2016), and protein (GB/T 5009.5 2016).

Yield in microfibrillated cellulose

A dilute suspension with 0.1% to 0.2% of solid content (S_c) was centrifuged at 4000 rpm for 20 min to separate the microfibrillated material (in supernatant fraction) from the non-fibrillated or partially fibrillated ones, which precipitate. The sediment fraction was dried to a constant weight at 90 °C in a halogen desiccator. The yield was calculated from Eq. 1, and the results represent the average values of the three replications.

$$\text{Yield\%} = (1 - (\text{weight of dried sediment})/(\text{weight of diluted sample} \times \%S_c)) \times 100 \qquad (1)$$

Fourier transform infrared (FTIR) spectroscopy

The chemical changes of SR, TSR, MFC-5, and MFC-25 were analyzed by FTIR spectroscopy. The samples were ground and mixed with KBr and then pressed into transparent thin pellets. The FTIR spectra were obtained on a Vertex70 Fourier transform infrared instrument (Bruker, Karlsruhe, Germany) in the range of 500 cm^{-1} to 4000 cm^{-1}.

X-ray powder diffraction (XRD) analysis

The crystalline phases of SR, TSR, MFC-5, and MFC-25 were investigated by using a D/max 2200PC powder diffractometer (Rigaku, Tokyo, Japan). Radial scans of intensity were recorded at ambient condition over scattering 2θ angles from 5° to 60° (step size = 0.02, scanning rate = 2 s/step) using a Ni-filtered Cu Kα radiation, an operating voltage of 45 kV, and a filament current of 40 mA. The crystallinity index (CrI) of each sample was calculated by referring to diffraction intensity of crystalline and amorphous regions using the following empirical equation (Segal *et al.* 1959),

$$\text{CrI}\ (\%) = (I_{200} - I_{am})/I_{200} \times 100 \tag{2}$$

where I_{200} is the peak intensity at plane (200) ($2\theta = 22.6°$), and I_{am} is the minimum intensity at the valley between plane (200) and (110) ($2\theta = 18.7°$).

SEM analysis

A scanning electron microscope (SEM) was used to characterize the morphology of SR, TSR, MFC-5, and MFC-25. After freeze-drying, the fibers were affixed to metal stubs using double-faced tape, and the surface was coated with gold using an ion sputter instrument. Images were recorded using a scanning electron microscope (S-4800, Hitachi, Tokyo, Japan), and analyzed by Nano Measurer software (Department of Chemistry, Fudan University, Shanghai, China).

Thermal characterization

The thermal stabilities of SR, TSR, MFC-5, and MFC-25 were evaluated using STA449F3-1053-M equipment (NETZSCH, Selb, Germany). The analysis conditions were a nitrogen atmosphere with flow 40 mL/min, heating rate of 10 °C/min, temperature range 25 °C to 600 °C, and sample mass between 3 mg and 5 mg.

RESULTS AND DISCUSSION

Chemical Composition

The original chemical composition (dry basis) of okara contained 72.13% holocellulose, 64.26% α-cellulose, 16.36% protein, 6.17% fat, 3.34% ash, and 1.14% lignin. Okara had the same holocellulose as wood fibers (70% to 80%) and other agricultural residues, such as rice straw (68.1%), bagasse (73.7%), and cotton stalk (71%) (Adel *et al.* 2016). Moreover, because okara had less lignin than wood fibers (20% to 35%), it was not necessary to remove as much lignin through cooking or bleaching processes to isolate MFC. However, it was vital to remove protein and fat for extraction of MFC from okara.

Upon chemical treatment, the cellulose content continuously increased as expected. Almost all of the fat content was removed during extraction with petroleum ether. The protease treatment was efficient in removing protein, which significantly decreased from 16.36% to 4.31% following treatment. Ash was removed during acid treatment (Chen *et al.* 2013), which decreased from 3.34% to 1.12%. After chemical treatment, lignin content was 1.08%, which was slightly lower than raw material content. The holocellulose and α-cellulose content were increased from 72.13% and 64.26% to 90.12% and 87.41% after acid treatment, respectively.

The increase in cellulose proportion was expected because the hemicelluloses were partially solubilized by acid treatment. Acid treatment of the okara increased the surface area of the fibers, which leads to polysaccharides that are more susceptible to degradation (Alemdar and Sain 2008). The change in the chemical composition of okara resulted in a better crystalline degree of cellulose and improved thermal properties of the fibers. This was similar to a previous report (Alemdar and Sain 2008).

The yields of MFC, with respect to the initial amount of dried TSR fibers, for MFC-5 and MFC-25 were 26.6% and 32.4 wt%, respectively; these values were smaller than yields reported for other non-woody fibers 40% to 50% (Alila *et al.* 2013). This may be because the amorphous region of okara cellulose was higher than other non-wood fibers. In this study, a gentle homogenization process was used (60 MPa press), which was much lower than the 300 Mpa used in prior studies (Alila *et al.* 2013). However, with the lower pressure used in homogeneous, less energy was consumed (Luo *et al.* 2007). These conditions were conducive to the commercialization of MFC.

Spectroscopic analysis

The chemical characteristics of all samples were analyzed by FTIR spectroscopy. The FTIR spectra of SR, TSR, MFC-5, and MFC-25 are shown in Fig. 1. The dominant peaks in the 3400 cm^{-1} to 3200 cm^{-1} region were observed in the spectra of all the okara fiber samples. These peaks corresponded to the O-H stretching vibration of the hydroxyl group in cellulose molecules and demonstrated the hydrophilic tendencies of the fibers (Mondragon *et al.* 2014). The peak became more intense and widened toward the higher wavenumber side with treatment. The absorption bands in the neighborhood of 2935 cm^{-1} were found in the spectra of all the C-H stretching vibration of the alkyl groups of celluloses (Fahma *et al.* 2011). The peak 1740 cm^{-1} in the spectrum of okara was attributed to the acetyl or uronic ester groups of hemicellulose in the raw fibers. This peak decreased in the spectrum of chemical treated okara, which could indicate the reduction of the amorphous part where most of acetyl groups were linked, and finally almost disappeared in the spectra of MFC-5 and MFC-25 because of chemi-mechanical treatment. Due to the hydrophilic nature of the samples, all fibers showed signals in the range of 1603 cm^{-1} to 1647 cm^{-1}; these absorbance features were attributed to water absorbed by the cellulose fiber structures (Fatah *et al.* 2014). The absorption maximum of the water peak was slightly shifted to a lower wave number and was enhanced in the spectrum of MFC-5 and MFC-25 (Chandra *et al.* 2016).

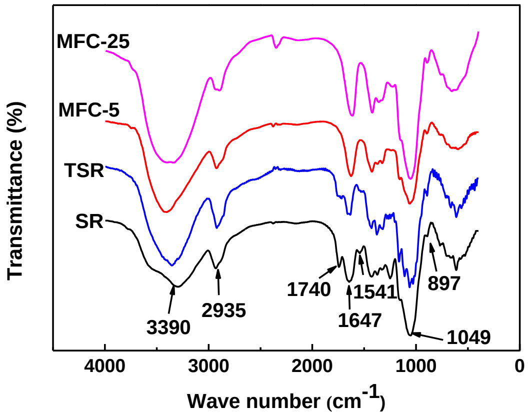

Fig. 1. FTIR spectra of SR, TSR, MFC-5 and MFC-25

Peaks in the range of 1500 cm^{-1} to 1660 cm^{-1} would indicate proteins. The peak at 1541 cm^{-1} in SR was attributed to the bending vibration of N-H; its absence indicated that the extracted MFC cellulose contained only an undetectable amount of proteins and had high purity (Xiang *et al.* 2016). The peaks at approximately 1375 cm^{-1} and 897 cm^{-1} were due to the O-H bending vibration and C-H deformation vibration of the cellulose. Apparently, no difference was found between the spectra of chemical treated and chemi-mechanical treated samples. The results suggested that mechanical treatments, such as homogenization, did not dramatically affect the chemical composition of the cellulose staring material (Turbak *et al.* 1983).

Crystalline Structures

The XRD patterns of SR, TSR, MFC-5, and MFC-25 were displayed in Fig. 2. The original sample SR showed a broad diffraction peak. When samples were treated by acid hydrochloric, a sharp diffraction peak was observed.

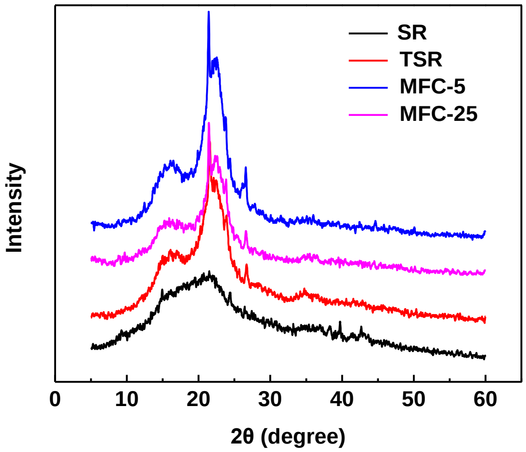

Fig. 2. X-ray diffraction patterns of SR, TSR, MFC-5, and MFC-25

The SR presented a less pronounced peak at $2\theta = 22^{o}$ because this sample had a much lower crystallinity index (14.6%) due to the presence of amorphous composition such as fat, protein, and aqueous soluble substances.

After purification and acid hydrolysis treatment, the crystallinity of TSR sample increased by 3.71 fold (to 54.2%). The purification and acid treatment removed non-cellulosic materials and disrupted hydrogen bonding in the cellulose structure to increase the crystal surface area and to reduce the amount of certain protein and fat that covered the outer surface of the fiber cell.

The higher CrI value of MFC compared with TSR was attributed to removal and reduction of the amorphous cellulose area and the further increase in the crystal surface area by mechanical treatment. The crystallinity index of MFC-5 and MFC-25 were 63.4% and 57.1%, respectively. These values were smaller than those found in other non-woody fibers (sisal 70%, abaca 67.5%, jute 72.5%, hemp 82%, and flax 79%) (Alila *et al.* 2013). This result was consistent with the previous yield of the MFC and was lower than other non-woody fibers. Thus, the crystallinity of okara was lower. However, a decrease in CrI of MFC-25 with respect to MFC-5 was observed, and this suggested that the homogenization of MFC-25 was severe under the mechanical conditions employed; therefore, the increasing times of pressure homogenization removed the amorphous portion of cellulose, partly destroyed the crystalline region, and produced new amorphous cellulose.

The X-ray diffractograms revealed that the major intensity peak was located at a 2θ value of around 15° (plane 101), 17° (plane 101), 21° (plane 021), 23° (plane 002), and 34° (plane 004), which were related to the crystalline structure of cellulose I for all samples (Borysiak and Garbarczyk 2003).

Morphology Analysis

The microstructures of SR, TSR, MFC-5, and MFC-25 are shown in Fig. 3. The SEM image of Fig. 3a showed that SR had an irregular particulate structure with different shape and size (about 10 µm to 40 µm in length and 5 µm to 20 µm in width). The SEM image of TSR taken to investigate its structure is shown in Fig. 3b. Visually, it was clear that TSR changed the structure completely. The modified morphology evidenced that acid treatment partially removed the amorphous compounds hemicellulose and protein, as well as other compounds present in the okara, such as lignin and fat. As a result of the flow during the pressurized homogeneous process, TSR was separated into much smaller cellulose products. The most common forms were the fibrillar and network nanostructure. These two different forms of MFC could not be separated by the general methods of centrifugation and filtration.

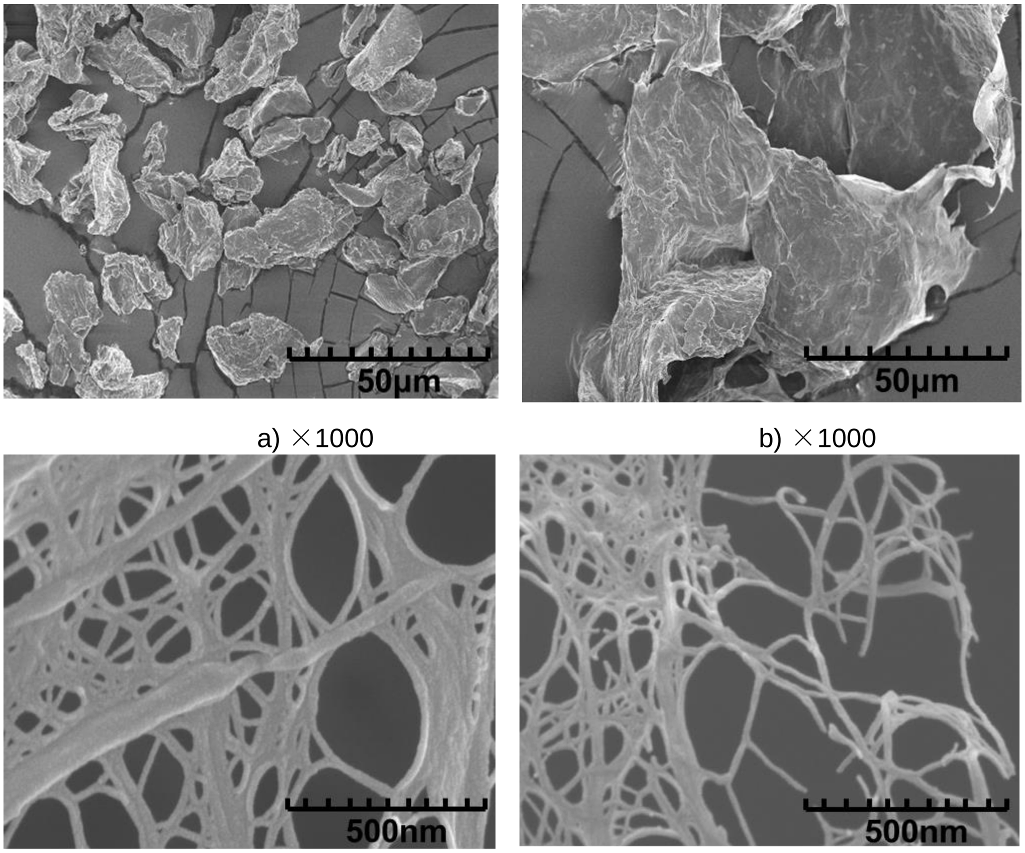

a) ×1000

b) ×1000

c) ×100000

d) ×100000

Fig. 3. SEM of the SR (a), TSR (b), MFC-5 (c) and MFC-25 (d)

When nanofibers were isolated, the main aim was to obtain nanoparticles measuring less than 100 nm, because larger length, smaller diameter, and more uniform particles are better for many applications of MFC, especially in composites (Tibolla *et al.* 2017). The diameter of the fibers after mechanical treatment were calculated from SEM images by an image processing analysis program. Figure 4 shows the statistics of the diameter of MFC-5and MFC-25. The diameter of the MFC-25 changed slightly compared with MFC-5. The diameter of 80% of the MFC-25 was smaller than 36 nm. The average diameter was between 13 nm and 18 nm, with 28% of the amounts occurring in this range. The diameter of MFC-5 ranged from 13 nm to 93 nm. Almost 30% of MFC-5 had a diameter with a range of 29 nm to 37 nm. The range of MFC from okara was similar to the size of the CNF obtained from sisal and abaca fibers (20 nm) (Abraham *et al.* 2011), hemp, jute, and flax fibers (30 nm to 50 nm) (Alila *et al.* 2013), bagasse pulp (9 nm to 25 nm) (Hassan *et al.* 2011), and rice straw (10 nm to 65 nm) (Hassan *et al.* 2012). The increase on homogenization time resulted in a slightly shorter diameter for MFC-25 when compared with MFC-5. This was expected, since the greater homogenization time partially destroyed areas of the crystalline domains, as can be seen from the XRD analysis.

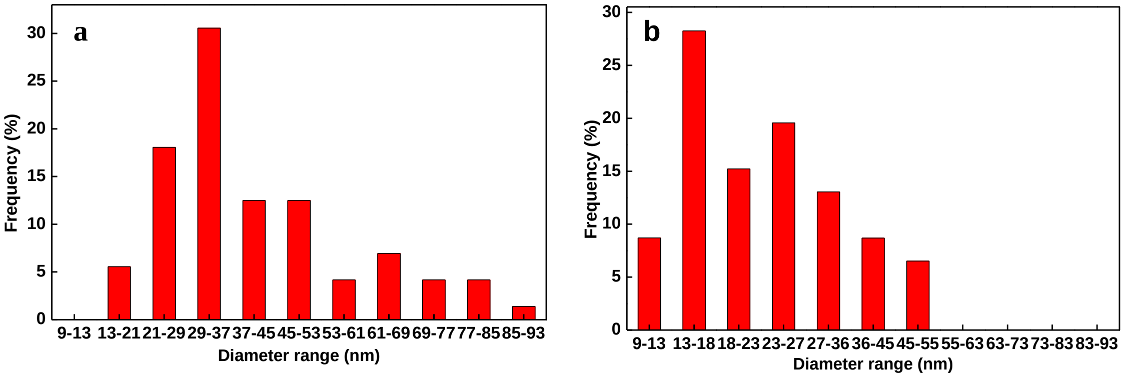

Fig. 4. Width distribution of the MFC-5 a and MFC-25 b

Thermogravimetric Analysis

Determining the thermal properties and thermal stability of the natural fibers is important for their potential use in the processing of biocomposities (Johar *et al.* 2012). For example, the main application of MFC is as a reinforcing agent in the nanocomposite field, for which it is processed at temperatures sufficient to melt thermoplastics, which can be above 200 °C.

Thermogravimetric (TG) and derivative thermogravimetry (DTG) curves of the SR, TSR, MFC-5, and MFC-25 are shown in Figs. 5a and 5b, respectively. There were three stages during thermal degradation, namely, low molecule weight compounds and water escape, cellulose degradation, and residue degradation. In all cases, the first stage exhibited a small weight loss in the range of 25 °C to 150 °C, due to the evaporation of the water and low molecular compounds (Kumar *et al.* 2014). The initial degradation temperatures were approximately 210 °C, 268 °C, 225 °C, and 248 °C, respectively. The initial degradation temperature of TSR (268 °C) was increased compared with the original SR (210 °C). Due to the low initial decomposition temperatures of fat, protein, and hemicellulose, the higher initial temperatures of thermal decomposition of TSR was related to the partial removal of non-cellulose by purification processes.

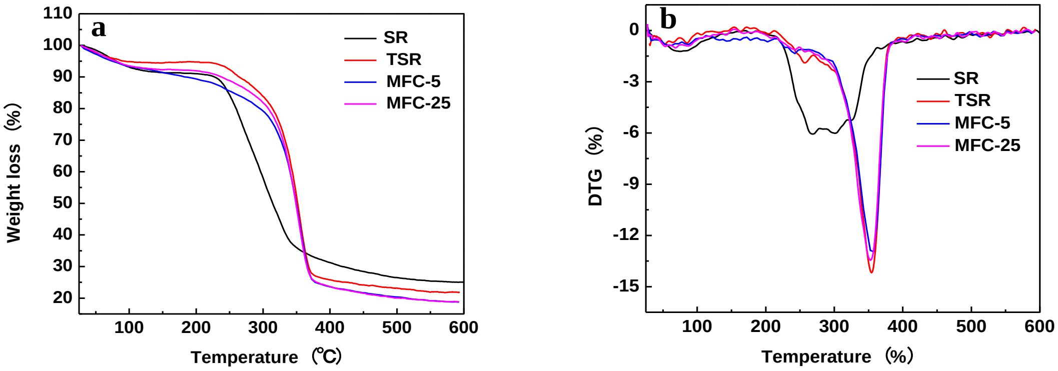

Fig. 5. TGA a and DTG b curves of SR, TSR, MFC-5, and MFC-25

The second stage was the thermal decomposition of cellulose from 200 °C to 400 °C included depolymerization, dehydration, and decomposition of glycosyl units (Roman and Winter 2004). Untreated okara started to decompose at around 210 °C, while acid hydrochloric treated okara started to decompose at around 300 °C. In addition, a peak was observed in the DTG curve of raw materials at around 268 °C, but it was no longer present after acid hydrochloric treatment, which was attributed to the partial removal of hemicellulose, fat, and protein by purification processes. The rate of degradation reached its peak at 268 °C and 301 °C, 350 °C, 355 °C, and 352 °C for the SR, TSR, MFC-5, and MFC-25, respectively.

The thermal stability of TSR, MFC-5, and MFC-25 was higher than that of the SR. The final stage above 400 °C was attributed to the oxidation and breakdown of charred residue to lower molecular weight gaseous products (Roman and Winter 2004). In this stage, the charred residue of the SR, TSR, MFC-5, and MFC-25 was 25.0%, 27.1%, 18.7%, and 18.8%, respectively. The decrease in charred residue of MFC-5 and MFC-25 was because MFC has the nano-sizes (the dimeter is less 100 nm) and higher surface area, which caused it to be more exposed to the effects of heating. Thus, the higher temperature of thermal decomposition and lesser residual mass of the fibers obtained after chemi-mechanical treatment was related to removal of fat, protein, and hemicelluloses from the okara and higher crystallinity of the cellulose.

Acid hydrolysis led to a remarkable increase in thermal stability of okara, but the initial degradation temperature of MFC-5 and MFC-25 were smaller than TSR. This result may be attributed to the increase in heat transfer rate due to the larger surface area of MFC. These results were very consistent with results obtained from the chemical composition, FTIR, and XRD measurements.

In sum, MFC extraction from okara represented an environmentally friendly approach with reduced use of purification, acid hydrochloric treatment, and gentle homogenization (low pressure). The MFC obtained from this experiment has been added to an agro-waste material as part of the generation of ecofriendly cellulosic nanofibrillated for diversified applications.

CONCLUSIONS

1. The amorphous region of okara cellulose was higher than other non-wood fibers. The required conditions of homogenization were relatively gentle (only 60 MPa), which is lower than the value 100 MPa used in other work. The diameters of MFC-5 and MFC-25 were within the range of 13 to 93 nm and 9 nm to 55 nm, respectively.
2. MFC obtained from okara had great potential as reinforcement in ecofriendly cellulosic nanofibrillated for diversified applications.

ACKNOWLEDGMENTS

The authors are grateful for the support of the China Scholarship Council and the financial support of the Project of Shaanxi Province Natural Science Basic Research, Grant No. 2015JM3118, the project of Tianjin Pulp and Paper Key Laboratory Open Fund, Grant. No. 201608, the project of Shaanxi Provincial Department of Education Key Laboratory Research Open Fund, Grant No. 17JS017, and the project of Shaanxi University of Science and Technology Research Initial Fund, Grant No. BJ15-29.

REFERENCES CITED

Abdulkhani, A., Alizadeh, P., Hedjazi, S., and Hamzeh, Y. (2017). “Potential of soya as a raw material for a whole crop biorefinery,” *Renewable and Sustainable Energy Reviews* 75, 1269-1280. DOI: 10.1016/j.rser.2016.10.082

Abraham, E., Deepa, B., Pothan, L. A., Jacob, M., Thomas, S., Cvelbar, U., and Anandjiwala, R. (2011). “Extraction of nanocellulose fibrils from lignocellulosic fibres: A novel approach,” *Carbohydrate Polymers* 86(4), 1468-1475. DOI: 10.1016/j.carbpol.2011.06.034

Adel, A. M., El-Gendy, A. A., Diab, M. A., Abou-Zeid, R. E., El-Zawawy, W. K., and Dufresne, A. (2016). “Microfibrillated cellulose from agricultural residues. Part I: Papermaking application,” *Industrial Crops and Products* 93, 161-174. DOI: 10.1016/j.indcrop.2016.04.043

Agoda-Tandjawa, G., Durand, S., Berot, S., Blassel, C., Gaillard, C., Garnier, C., and Doublier, J.-L. (2010). “Rheological characterization of microfibrillated cellulose suspensions after freezing,” *Carbohydrate Polymers* 80(3), 677-686. DOI: 10.1016/j.carbpol.2009.11.045

Alemdar, A., and Sain, M. (2008). “Isolation and characterization of nanofibers from agricultural residues – Wheat straw and soy hulls,” *Bioresource Technology* 99(6), 1664-1671. DOI: 10.1016/j.biortech.2007.04.029

Alila, S., Besbes, I., Vilar, M. R., Mutjé, P., and Boufi, S. (2013). “Non-woody plants as raw materials for production of microfibrillated cellulose (MFC): A comparative study,” *Industrial Crops and Products* 41, 250-259. DOI: 10.1016/j.indcrop.2012.04.028

Borysiak, S., and Garbarczyk, J. (2003). “Applying the WAXS method to estimate the supermolecular structure of cellulose fibers after mercerization,” *Fibers and Textiles in Eastern Europe* 11(5), 104-106.

Chandra, J., George, N., and Narayanankutty, S. K. (2016). "Isolation and characterization of cellulose nanofibrils from arecanut husk fibre," *Carbohydrate Polymers* 142, 158-166. DOI: 10.1016/j.carbpol.2016.01.015

Chen, Q., Huang, L., Chen, L., and Chen, Y. (2013). "Study on acid treatment process and the impact on fiber properties of bamboo dissolving pulp," *Chemical Engineering and Equipment* 3, 004.

Eichhorn, S. J., Dufresne, A., Aranguren, M., Marcovich, N. E., Capadona, J. R., Rowan, S. J., Weder, C., Thielemans, W., Roman, M., Renneckar, S., Gindl, W., Veigel, S., Keckes, J., Yano, H., Abe, K., Nogi, M., Nakagaito, A. N., Mangalam, A., Simonsen, J., Benight, A. S., Bismarck, A., Berglund, L. A., and Peijs, T. (2010). "Review: Current international research into cellulose nanofibres and nanocomposites," *Journal of Materials Science* 45(1), 1-33.

Fahma, F., Iwamoto, S., Hori, N., Iwata, T., and Takemura, A. (2011). "Effect of pre-acid-hydrolysis treatment on morphology and properties of cellulose nanowhiskers from coconut husk," *Cellulose* 18(2), 443-450. DOI: 10.1007/s10570-010-9480-0

Fatah, I. Y. A., Khalil, H., Hossain, M. S., Aziz, A. A., Davoudpour, Y., Dungani, R., and Bhat, A. (2014). "Exploration of a chemo-mechanical technique for the isolation of nanofibrillated cellulosic fiber from oil palm empty fruit bunch as a reinforcing agent in composites materials," *Polymers* 6(10), 2611-2624. DOI: 10.3390/polym6102611

Ferguson, W. (2012). "Wood pulp is surprise new wonder material," *New Scientist* 215(2878), 24-24.

GB/T 5009.5 (2016). "Protein in food," Standardization Administration of China, Beijing, China.

GB/T 5009.6 (2016). "Protein in food," Standardization Administration of China, Beijing, China.

Habibi, Y., Mahrouz, M., and Vignon, M. R. (2009). "Microfibrillated cellulose from the peel of prickly pear fruits," *Food Chemistry* 115(2), 423-429. DOI: 10.1016/j.foodchem.2008.12.034

Hassan, E. A., Hassan, M. L., and Oksman, K. (2011). "Improving bagasse pulp paper sheet properties with microfibrillated cellulose isolated from xylanase-treated bagasse," *Wood and Fiber Science* 43(1), 76-82.

Hassan, M. L. (2015). "Bagasse and rice straw nanocellulosic materials and their applications," in: *Handbook of Polymer Nanocomposites. Processing, Performance and Application*, Springer, New York, pp. 47-64.

Hassan, M. L., Mathew, A. P., Hassan, E. A., El-Wakil, N. A., and Oksman, K. (2012). "Nanofibers from bagasse and rice straw: Process optimization and properties," *Wood Science and Technology* 46(1-3), 193-205. DOI: 10.1007/s00226-010-0373-z

Henniges, U., Veigel, S., Lems, E. -M., Bauer, A., Keckes, J., Pinkl, S., and Gindl-Altmutter, W. (2014). "Microfibrillated cellulose and cellulose nanopaper from *Miscanthus* biogas production residue," *Cellulose* 21(3), 1601-1610.

Jimat, D. N., and Zailani, I. S. (2016). "Comparison study on characteristics of microfibrillated cellulose (MFC) extracted from cocoa pod husk and sugarcane bagasse," in: *4th International Conference on Biotechnology Engineering 2016*, Kuala Lumpur, Malaysia.

Johar, N., Ahmad, I., and Dufresne, A. (2012). "Extraction, preparation and characterization of cellulose fibres and nanocrystals from rice husk," *Industrial Crops and Products* 37(1), 93-99. DOI: 10.1016/j.indcrop.2011.12.016

Klemm, D., Kramer, F., Moritz, S., Lindstrom, T., Ankerfors, M., Gray, D., and Dorris, A. (2011). "Nanocelluloses: A new family of nature-based materials," *Angewandte Chemie-International Edition* 50(24), 5438-5466. DOI: 10.1002/anie.201001273

Kumar, A., Negi, Y. S., Choudhary, V., and Bhardwaj, N. K. (2014). "Characterization of cellulose nanocrystals produced by acid-hydrolysis from sugarcane bagasse as agro-waste," *Journal of Materials Physics and Chemistry* 2(1), 1-8. DOI: 10.1007/978-3-642-27758-0_1162-2

Lavoine, N., Desloges, I., Dufresne, A., and Bras, J. (2012). "Microfibrillated cellulose– Its barrier properties and applications in cellulosic materials: A review," *Carbohydrate Polymers* 90(2), 735-764. DOI: 10.1016/j.carbpol.2012.05.026

Liu, L.-L., Tian, Y.-B., and Liu, X. (2012). "Physico-chemical properties and characterization of nano-crystalline soybean dregs cellulose," *Food Science* 33(9), 41-46.

Luo, Y.-Z., Lu, Y.-Q., and Wang, W.-L. (2007). "Principle and application of homogenizer," *China Dairy Industry* 10, 018.

Missoum, K., Martoïa, F., Belgacem, M. N., and Bras, J. (2013). "Effect of chemically modified nanofibrillated cellulose addition on the properties of fiber-based materials," *Industrial Crops and Products* 48, 98-105. DOI: 10.1016/j.indcrop.2013.04.013

Mondragon, G., Fernandes, S., Retegi, A., Peña, C., Algar, I., Eceiza, A., and Arbelaiz, A. (2014). "A common strategy to extracting cellulose nanoentities from different plants," *Industrial Crops and Products* 55, 140-148. DOI: 10.1016/j.indcrop.2014.02.014

Nyström, G., Marais, A., Karabulut, E., Wågberg, L., Cui, Y., and Hamedi, M. M. (2015). "Self-assembled three-dimensional and compressible interdigitated thin-film supercapacitors and batteries," *Nature Communications* 6(7259). DOI: 10.1038/ncomms8259.

Petroudy, S. R. D., Syverud, K., Chinga-Carrasco, G., Ghasemain, A., and Resalati, H. (2014). "Effects of bagasse microfibrillated cellulose and cationic polyacrylamide on key properties of bagasse paper," *Carbohydrate Polymers* 99, 311-318. DOI: 10.1016/j.carbpol.2013.07.073

Roman, M., and Winter, W. T. (2004). "Effect of sulfate groups from sulfuric acid hydrolysis on the thermal degradation behavior of bacterial cellulose," *Biomacromolecules* 5(5), 1671-1677. DOI: 10.1021/bm034519+

Segal, L., Creely, J., Martin Jr., A., and Conrad, C. (1959). "An empirical method for estimating the degree of crystallinity of native cellulose using the X-ray diffractometer," *Textile Research Journal* 29(10), 786-794.

Shi, Z., Yang, Q., Ono, Y., Funahashi, R., Saito, T., and Isogai, A. (2015). "Creation of a new material stream from Japanese cedar resources to cellulose nanofibrils," *Reactive and Functional Polymers* 95, 19-24. DOI: 10.1016/j.reactfunctpolym.2015.08.005

Shogren, R. L., Peterson, S. C., Evans, K. O., and Kenar, J. A. (2011). "Preparation and characterization of cellulose gels from corn cobs," *Carbohydrate Polymers* 86(3), 1351-1357. DOI: 10.1016/j.carbpol.2011.06.035

Singh, M., Kaushik, A., and Ahuja, D. (2016). "Surface functionalization of nanofibrillated cellulose extracted from wheat straw: Effect of process parameters," *Carbohydrate Polymers* 150, 48-56. DOI: 10.1016/j.carbpol.2016.04.109

Spence, K. L., Venditti, R. A., Habibi, Y., Rojas, O. J., and Pawlak, J. J. (2010a). "The effect of chemical composition on microfibrillar cellulose films from wood pulps:

Mechanical processing and physical properties," *Bioresource Technology* 101(15), 5961-5968. DOI: 10.1016/j.biortech.2010.02.104

Spence, K. L., Venditti, R. A., Rojas, O. J., Habibi, Y., and Pawlak, J. J. (2010b). "The effect of chemical composition on microfibrillar cellulose films from wood pulps: Water interactions and physical properties for packaging applications," *Cellulose* 17(4), 835-848. DOI: 10.1007/s10570-010-9424-8

Syverud, K., Kirsebom, H., Hajizadeh, S., and Chinga-Carrasco, G. (2011). "Cross-linking cellulose nanofibrils for potential elastic cryo-structured gels," *Nanoscale Research Letters* 6(1), 626. DOI: 10.1186/1556-276X-6-626

TAPPI T211 om-02 (2011). "Ash in wood and pulp," TAPPI Press, Atlanta, GA.

TAPPI T222 om-11 (2011). "Acid-insoluble lignin in wood and pulp," TAPPI Press, Atlanta, GA.

Tibolla, H., Pelissari, F. M., Rodrigues, M. I., and Menegalli, F. C. (2017). "Cellulose nanofibers produced from banana peel by enzymatic treatment: Study of process conditions," *Industrial Crops and Products* 95, 664-674. DOI: 10.1016/j.indcrop.2016.11.035

Turbak, A. F., Snyder, F. W., and Sandberg, K. R. (1983). "Suspensions containing microfibrillated cellulose," U. S. Patent No. 4487634A.

Vartiainen, J., Pöhler, T., Sirola, K., Pylkkänen, L., Alenius, H., Hokkinen, J., Tapper, U., Lahtinen, P., Kapanen, A., and Putkisto, K. (2011). "Health and environmental safety aspects of friction grinding and spray drying of microfibrillated cellulose," *Cellulose* 18(3), 775-786. DOI: 10.1007/s10570-011-9501-7

Vong, W. C. and Liu, S.-Q. (2016). "Biovalorisation of okara (soybean residue) for food and nutrition," *Trends in Food Science and Technology* 52, 139-147. DOI: 10.1016/j.tifs.2016.04.011

Vong, W. C. and Liu, S.-Q. (2017). "Changes in volatile profile of soybean residue (okara) upon solid-state fermentation by yeasts," *Journal of the Science of Food and Agriculture* 97(1), 135-143. DOI: 10.1002/jsfa.7700

Xhanari, K., Syverud, K., and Stenius, P. 2011. "Emulsions stabilized by microfibrillated cellulose: The effect of hydrophobization, concentration and o/w ratio," *Journal of Dispersion Science and Technology* 32(3), 447-452. DOI: 10.1080/01932691003658942

Xiang, Z., Gao, W., Chen, L., Lan, W., Zhu, J., and Runge, T. (2016). "A comparison of cellulose nanofibrils produced from *Cladophora glomerata* algae and bleached eucalyptus pulp," *Cellulose* 23(1), 493-503. DOI: 10.1007/s10570-015-0840-7

Zhang, X., Yu, Y., Li, W., Ren, D., and Wang, H. (2015). "An efficient dispersive agent—KCl for ultrasonic preparation of microfibrillated cellulose (MFC)," *BioResources* 10(4), 6635-6642. DOI: 10.15376/biores.10.4.6635-6642

Zhao, Y., Han, J.-C., Zheng, H.-Y., Xu, H., and Xu, L.-F. (2013). "Research of further processing and comprehensive utilization of soybean dregs," *Soybean Science* 4, 027.

Zobel, B. J., and McElwee, R. L. (1958). "Variation of cellulose in loblolly pine," *TAPPI* 41(4), 167-70.

Article submitted: June 2, 2018; Peer review completed: July 28, 2018; Revised version received: August 19, 2018; Accepted: August 20, 2018; Published: September 4, 2018. DOI: 10.15376/biores.13.4.7944-7956